Nanomed. J. 4(3): 135-141, Summer 2017

RESEARCH PAPER

The effect of mesoporous silica nanoparticles loaded with epirubicin on drug-resistant cancer cells

Mohammad Yahya Hanafi-Bojd [1], Legha Ansari [2], Fatemeh Mosaffa [3], Bizhan Malaekeh-Nikouei [4]*

[1]Cellular and Molecular Research Center, Department of Pharmacology, School of Medicine, Birjand University of Medical Sciences, Birjand, Iran

[2]School of Pharmacy, Mashhad University of Medical Sciences, Mashhad, Iran

[3]Department of Pharmaceutical Biotechnology, School of Pharmacy, Mashhad University of Medical Sciences, Mashhad, Iran

[4]Nanotechnology Research Center, School of Pharmacy, Mashhad University of Medical Sciences, Mashhad, Iran

ABSTRACT

Objective (s): In chemotherapy for cancer treatment, the cell resistance to multiple anticancer drugs is the major clinical problem. In the present study, mesoporous silica nanoparticles (MSNs) were used as a carrier for epirubicin (EPI) in order to improve the cytotoxic efficacy of this drug against the P-glycoprotein (P-gp) overexpressing cell line.

Materials and Methods: MSNs with phosphonate groups were synthesized and characterized. The cytotoxicity of the prepared nanoparticles on drug-sensitive human breast cancer cell line (MCF-7) and drug-resistant cancer cells (MCF-7/ADR) was evaluated.

Results: The hydrodynamic size of nanoparticles was 98 nm and surface charge was negative. The viability of sensitive MCF-7 and resistant MCF-7/ADR cells after incubation with MSNs containing EPI at concentration of 5 µg/ml was about 75% and 44%. On the other hand, the viability of sensitive and resistant cells after incubation with free EPI at this concentration was about 48% and 60%, respectively.

Conclusion: These nanoparticles exhibited suitable drug efficiencies against drug-resistant MCF-7/ADR cells in *in vitro* experiments.

Keywords: *Epirubicin, Mesoporous silica nanoparticles, Multi drug resistance, P-glycoprotein*

How to cite this article

Hanafi-Bojd MY, Ansari L, Mosaffa F, Malaekeh-Nikouei B. The effect of mesoporous silica nanoparticles loaded with epirubicin on drug-resistant cancer cells. Nanomed J. 2017; 4(3):135-141. DOI: 10.22038/nmj.2017.8954

INTRODUCTION

Cancer is one of the main reasons of death, and chemotherapy is one of the most common cancer treatment approach that uses chemotherapeutic agents to kill cancer cells [1, 2]. The major impediment in chemotherapy cancer treatment is multi drug resistance (MDR). This resistance mechanistically is related to the adenosine triphosphate (ATP)-binding cassette (ABC) transporters such as P-glycoprotein (P-gp or ABCB1). These transporters are located in the cell membrane and their function is pumping drugs out of cancer cells, forming drug efflux. Therefore, the intracellular concentration of drugs is reduced that in turn, leading to drug resistance [3, 4]. Several strategies have been developed to overcome this hurdle. Recently, nanoparticles have attracted increasing attention in drug delivery fields. Nanoparticulate drug delivery systems (NDDSs) have been proposed to execute "efflux circumventing strategy" to overcome MDR by intracellular drug delivery [5-8]. Upon arriving at tumor regions through enhanced permeability and retention (EPR) effects, NDDSs

* *Corresponding Author Email: malaekehb@mums.ac.ir*

Note. This manuscript was submitted on April 12, 2017; approved on May 23, 2017

are uptake by tumor cells and transported into endosomal compartments, that are in perinuclear regions physically away from the membrane ABC transporters [9]. This location advantage allows drugs released within these endosomal compartments to evade the efflux pumping, acting to kill tumor cells [3, 10-15].

Over the past decades, several nanoparticles have been developed and applied for targeted drug delivery to cancer cells, such as liposomes [16-21], polymeric micelles [22-25], dendrimers [26-28], carbon nanotubes [29-32], inorganic nanoparticles [33-36], nanographene [37, 38] and silica-based materials [39-43].

Mesoporous silica nanoparticles (MSNs) have attracted much attention due to their unique physiochemical properties, including large specific surface area and high pore volume, controllable particle size, easy surface modification, considerable stability and biocompatibility, and high drug-loading capacity. In 1992, scientists succeeded to synthesize ordered mesoporous silica nanomaterials for the first time. This discovery in material science lead to a diversity of applications ranging from food manufacturing to pharmaceutical technology [44]. In 2001, Vallet-Regí *et al* reported the application of MSNs as a delivery system for ibuprofen for the first time. They showed that up to 30 wt% of this drug could be loaded into the nanoparticles and sustained drug release from MSNs [45]. In 2015, Malaekeh-Nikouei and coworkers used functionalized MSNs for delivery of epirubicin (EPI). They proved that phosphonated MSNs have suitable pH-dependent release pattern as at pH=5.5 about 70% of EPI was released from MSNs in 24 h, while at pH=7.2, the amount of drug release dropped down to about 8% at the same time [41].

In the present study, we synthesized and functionalized MSNs by phosphonate group in order to achieve in negatively charged nanoparticles. The negative surface charge of MSNs and the mesoporous nature of these nanoparticles would allow good encapsulation of positively charged EPI. After that, we evaluated the cytotoxicity of the prepared nanoparticles on drug-sensitive human breast cancer cell line (MCF-7) and drug-resistant cancer cells (MCF-7/ADR**)**.

MATERIALS AND METHODS

Tetraethylorthosilicate (TEOS), 3- (trihydroxysilyl) propyl methylphosphonate (42%), cetyltrimethylammonium bromide (CTAB) and Pluronic®F127 were purchased from Sigma-Aldrich (USA). Cell culture medium RPMI 1640, fetal bovine serum (FBS) and penicillin/streptomycin were obtained from Gibco (USA).

Synthesis and functionalization of MSNs

The synthesis was performed as described in our previous study [41]. Briefly, deionized water and NaOH (2 M) were mixed. Then, Pluronic® F127 and CTAB were dissolved in this solution. This mixture was heated to 80 °C under stirring. After 30 min, TEOS was added into the solution. 20 min later, under argon atmosphere, the 3-(trihydroxysilyl) propyl methylphosphonate was added to the solution and stirred for another 2 h at 80 °C. Finally, the solution was cooled down to room temperature to obtain phosphonated MSNs (Ph-MSNs).

Surfactant removal

For removing of CTAB, dialysis method was used as follows. After nanoparticles synthesis, 30 ml of Ph-MSN nanoparticles suspension was transferred to a dialysis tube and dialyzed for 24 h against a mixture containing water:ethanol (50:50) and HCl. Next, Ph-MSNs were dialyzed against double distilled water for another 24 h and this process repeated twice [46, 47].

Characterization of MSNs

In order to determine the shape and structure, the nanoparticles were subjected to transmission electron microscopy (TEM) at 120 kV (LEO 912AB Zeiss electron microscope-Germany). One droplet of ethanolic dispersion of nanoparticles was placed on the carbon-coated copper grid and dried at room temperature. The particle size and zeta potential of the samples were determined by the Zetasizer (Nano-ZS, Malvern, UK) after dilution with deionized water.

For determination of carbon, hydrogen and nitrogen content, elemental analysis was carried out. Measurements were done using Costech ECS 4010 (Italy). FTIR spectroscopy was carried out using a Perkin–Elmer (USA) in the absorption mode in the range of 4000–450 cm^{-1}.

Drug loading

Drug loading was carried out as follows. 1 mg of Ph-MSNs was dispersed in 0.5 ml of EPI solution (2 mg/ml) and stirred for 24 h in dark environment

at room temperature. After that, Ph-MSNs were centrifuged and washed with deionized water to remove free drug molecules. To determine EPI loading efficiency, the fluorescence of the EPI supernatant and washed solutions was measured (ex: 488 nm/ em: 555 nm) in a microplate reader (Synergy H4- Hybrid, USA). The EPI content was calculated using a serial dilutions of EPI and eventually the drug loading content and drug loading efficiency were calculated as follows:

Drug loading content=(weight of loaded drug in Ph-MSNs/weight of drug and Ph-MSNs) ×100%

Drug loading efficiency= (weight of loaded drug in Ph-MSNs/weight of feeding drug)×100%

Cell Culture

Drug-sensitive human breast cancer cell line (MCF-7) and drug-resistant cancer cells (MCF-7/ADR) were cultured in complete medium (RPMI-1640 medium supplemented with 10% FBS, 100 U/ml penicillin, and 100 µg/ml streptomycin) and maintained at 37 °C in a humidified media and 5% CO_2 incubator.

Evaluation of Ph-MSN and cell viability

In vitro biocompatibility of Ph-MSNs and cytotoxicity of EPI-loaded Ph-MSNs (Ph-MSNs-EPI) was measured using the MTT viability assay. Cells were seeded in 96-well plates at a density of 5×10^3 cells per well in 100 µl of complete medium and incubated for 24 h. The cells were incubated with Ph-MSNs, Ph-MSNs-EPI and free EPI at different concentrations for 72 h. After the incubation, the MTT assay was performed by removing the medium and adding of 180 µl of fresh medium and 20 µl of MTT solution (5 mg/ml in PBS). The plates were incubated for 4 h at 37 °C. Subsequently, the medium was carefully removed, and then 200 µl of dimethyl sulfoxide (DMSO) was added to each well in order to dissolve the cells and MTT formazan. The plates were gently shaken for 5 min, and the absorbance of the obtained DMSO solution was determined at 570 nm by the microplate reader (Synergy H4-Hybrid, USA). The untreated cells were considered as control with 100% viability [48]. The viability of cells was calculated as follows.

Viability= (Absorbance of each well/Average of absorbance of control wells) ×100

Data analysis

Every experiment was repeated at least three times. IC_{50} values were achieved using Prism (GraphPad software, San Diego, CA).

RESULTS AND DISCUSSION

Synthesis and characterization of MSNs

MSNs are promising inorganic nanoparticles to deliver hydrophilic and hydrophobic anticancer drugs, gene, and siRNA into different cancer cell lines [49]. Because of their intrinsic high stability, excellent biocompatibility, and good degradability, these nanoparticles exhibited great potential to overcome MDR [50, 51]. Herein we used this inorganic carrier to improve antitumor efficacy of EPI. MSNs were synthesized and modified to possess phosphonate groups on its surface, forming the phosphonate functionalized MSNs (Ph-MSNs), followed by the template extraction using a dialysis method. The mean nanoparticles size and zeta potential were measured in deionized water. In order to achieve smaller and more stable Ph-MSNs in aqueous media for biological applications, we used CTAB and Pluronic® F127 as templating agents to reach better nanoparticles. This synthesis approach is very effective in obtaining smaller and monodispersed nanoparticles [41]. The hydrodynamic size of Ph-MSNs was 98.1±5.2 nm and the conjugation of phosphonate groups onto the surface of MSNs donates a high negative charge to the nanoparticles (-19.5± 0.6 mV). Regarding the positive charge of CTAB, the negative zeta potential of nanoparticles revealed that the CTAB removed successfully from the structure. The porous structure and size of Ph-MSNs were characterized using TEM. As shown in Fig. 1, the morphology was nearly spherical. FTIR spectrum showed typical peaks of silica nanoparticles (Fig. 2). The peaks at 1078 cm^{-1}, 802 cm^{-1} and 467 cm^{-1} are pertaining to Si–O–Si and Si–O. The peak at 952 cm^{-1} attributed to the vibration band of Si–OH. Also a broad peak around 3300 cm^{-1} is related to adsorbed water and Si–OH groups on the surface of MSNs.

The results achieved by elemental analysis are another evidences for the removal of CTAB from the pore of nanoparticles. Elemental analysis showed that most of CTAB was removed from the structure as the nitrogen content was very low (Table 1).

Table 1. Elemental analysis of Ph-MSN (the weight % of C, H and N is presented)

Elemental composition of Ph-MSN (Wt%)		
C	H	N
23.71	5.09	0.26

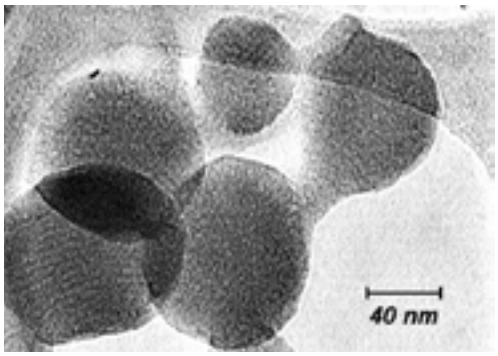

Fig. 1. Tem image of Ph-MSNs

EPI loading

EPI, an antitumor drug, was selected as a model drug and penetrated into the pores of Ph-MSNs by soaking nanoparticles in a solution of EPI. The electrostatic interaction between positively charged EPI and negatively charged Ph-MSNs is the driving force of the loading process. The loading content and loading efficiency of Ph-MSNs were 9.45% and 18.90%, respectively.

In vitro cytotoxicity of Ph-MSNs

In order to study the efficiency of EPI loaded Ph-MSNs, the standard MTT assay was carried out to assess the cellular viability of MCF-7 cells. Free EPI was set as positive control. As shown in Table 2, in sensitive cell lines, the IC_{50} of free EPI was lower than the IC_{50} of Ph-MSN-EPI, indicating that free-EPI is marginally more effective than Ph-MSN-EPI, likely due to EPI's higher water solubility and consequently higher cellular uptake [52].

The major barrier to the successful chemotherapy is MDR which is mainly related to drug efflux from cancer cells mediated by P-gp. P-gp is overexpressed in many human cancers, which exports drugs from the cells and resulted in reduction of the effective concentration of intracellular drug, that in turn lead to the failure of therapy. However, it is important to note that the theoretic and crystallography studies showed that the molecular size of P-gp is ~160 A° long and 45 × 65A° wide, with the core consisting of two nucleotide binding domains (NBDs) and two transmembrane domains (TMDs). The residues in transmembrane segments form a funnel-shaped drug-binding domain, which is narrow at the cytoplasmic side, wide at the extracellular side and 9~25 A° in the middle. Because of this unique feature, macromolecules such as some kinds of proteins remain effective against MDR, due to the large size of protein molecules impedes pumping them out by the P-gp [53-55]. Accordingly, we synthesized Ph-MSNs with the size of 98 nm to deliver EPI to MDR cells, with the aim of overcoming MDR. On the other hand, we anticipated that after cellular internalization, EPI loaded Ph-MSNs rapidly enter lysosomes in the perinuclear regions, which are far away from P-gp transporters in the resistant cell lines thus possibly bypassing drug efflux [56].

MCF-7 is a drug-sensitive human breast cancer cell line, and MCF-7/ADR is its drug-resistant counterpart, that is widely used as the MDR experimental model cell line because of its high expression level of P-gp [57, 58]. The MTT assay showed that the cell viability was still over 60% after treatment with 5 µg/ml EPI, which proved the resistance of MCF-7/ADR cells to EPI (Fig. 3). Therefore, we selected the resistant cell line MCF-7/ADR to determine whether MSNs containing EPI could reverse MDR. Through MTT assay, IC_{50} values of EPI and MSNs containing EPI against the sensitive MCF-7 cells and resistant MCF-7/ADR cells were evaluated and thereby the drug resistance index (DRI) was calculated and listed

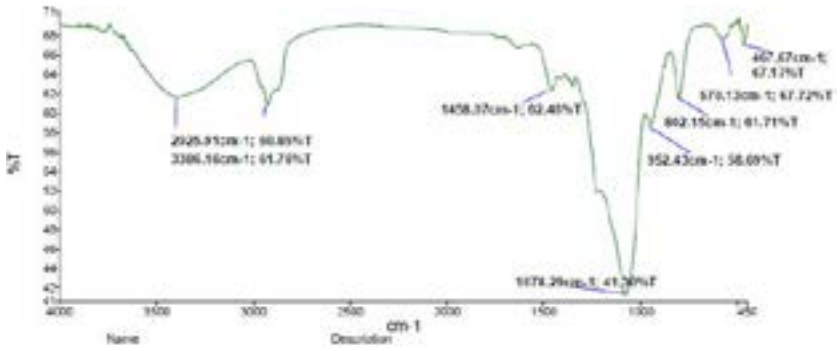

Fig. 2. FTIR spectrum of MSNs

Table 2. The IC50 values and DRI of EPI loaded Ph-MSN after incubation with MCF-7 and MCF-7/ADR cells for 72

Treatment type	TIME (h)	IC_{50}		DRI
		MCF-7	MCF-7/ADR	
EPI	72	1.884	7.466	3.963
MSNs containing EPI	72	8.705	4.854	1.79

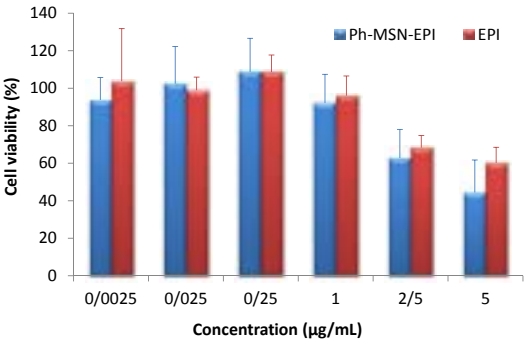

Fig. 3. The cell viability of MCF-7/ADR after 72h incubation with EPI and Ph-MSN-PI at different concentrations

in Table 2. The DRI value suggests a level of drug-resistance of the MCF-7/ADR cell compared to its counterpart sensitive cell MCF-7 (59). According to the DRI value, cancer cells can be classified into three categories: drug-sensitive one with DRI ranging from 0 to 2, moderate drug-resistant one with DRI from 2 to 10, and highly drug-resistant one with DRI higher than 10 [59, 60]. From DRI point of view, the DRI value in the EPI treated breast cancer cells is 3.963 for 72 h incubation, manifesting moderate drug-resistant cancer cells. For MSNs containing EPI (Ph-MSN-EPI), the IC_{50} value of EPI against sensitive MCF-7 cells is 8.705 µg/ml for 72 h incubation, while that against resistant MCF-7/ADR cells is 4.854 µg/ml (72 h), which is around 2-fold decrease over that of EPI. The DRI value for MSNs containing EPI (Ph-MSN-EPI) after 72 h incubation was 1.8. The values of IC_{50} and DRI indicate that MSNs containing EPI treated the moderate resistant MCF-7/ADR as sensitive drug-resistant cancer cells (Fig. 4 and Table 2).

The viability of sensitive MCF-7 and resistant MCF-7/ADR cells after incubation with pH-MSN-EPI at concentration of 5µg/ml was about 75% and 44%, respectively. On the other hand, the viability of sensitive MCF-7 and resistant MCF-7/ADR cells after incubation with EPI at concentration of 5 µg/ml was about 48% and 60%, respectively (Fig. 3 and Fig. 4). These results proved that the MSNs containing EPI are more effective on resistance

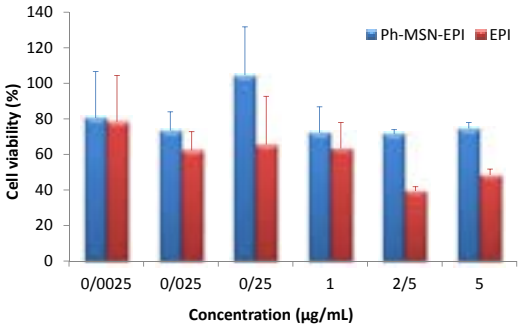

Fig. 4. The cell viability of MCF-7 after 72h incubation with EPI and Ph-MSN-PI at different concentrations

cells than sensitive cells. In addition, the MSNs containing EPI but not EPI were capable of effectively killing drug-resistant cells.

Therefore, all of these results indicate that MSNs containing EPI are a good candidate for effectively cancer drug resistance reversal. Probably, one can attribute it to the size-exclusion effect of P-gp, as small drug molecules can easily pump out of cell, whereas, nanoparticles remain inside.

CONCLUSION

In the present study, in order to achieve effective drug-resistance reversal, we have developed the MSN based drug delivery system to deliver EPI. Surface functionalization of MSNs with phosphonate group reduces nanoparticles aggregation due to electrostatic repulsion of negatively charged phosphonate groups on the surface of MSNs. Considering the size of these nanoparticles, the drug loaded MSNs showed acceptable toxicity against moderate resistant cancer cell line MCF-7/ADR. Although further efforts are necessary to reveal the exact efficacy of these nanoparticles for MDR cancer treatment, but this study suggests that MSNs containing EPI could serve as a practical example to overcome MDR.

ACKNOWLEDGMENTS

This study was supported by a Grant from the Vice Chancellor for Research of Mashhad University of Medical Science, Mashhad, Iran.

CONFLICT OF INTEREST

There is no conflict of interest in this study.

REFERENCES

1.Wang Z, Huang P, Jacobson O, Wang Z, Liu Y, Lin L, Lin J, Lu

N, Zhang H, Tian R. Biomineralization-inspired synthesis of copper sulfide–ferritin nanocages as cancer theranostics. ACS Nano. 2016; 10(3): 3453-3460.
2.Chabner BA, Roberts TG. Chemotherapy and the war on cancer. Nat Rev Cancer. 2005; 5(1): 65-72.
3.Zahreddine H, Borden K. Mechanisms and insights into drug resistance in cancer. Front Pharmacol. 2013; 4: 28.
4.Szakács G, Paterson JK, Ludwig JA, Booth-Genthe C, Gottesman MM. Targeting multidrug resistance in cancer. Nat Rev Drug Discov. 2006; 5(3): 219-234.
5.Markman JL, Rekechenetskiy A, Holler E, Ljubimova JY. Nanomedicine therapeutic approaches to overcome cancer drug resistance. Adv Drug Deliv Rev. 2013; 65(13): 1866-1879.
6.Shapira A, Livney YD, Broxterman HJ, Assaraf YG. Nanomedicine for targeted cancer therapy: towards the overcoming of drug resistance. Drug Resist Updat. 2011; 14(3): 150-163.
7.Pan L, Liu J, He Q, Wang L, Shi J. Overcoming multidrug resistance of cancer cells by direct intranuclear drug delivery using TAT-conjugated mesoporous silica nanoparticles. Biomaterials. 2013; 34(11): 2719-2730.
8.Qu Q, Ma X, Zhao Y. Targeted delivery of doxorubicin to mitochondria using mesoporous silica nanoparticle nanocarriers. Nanoscale. 2015; 7(40): 16677-16686.
9.Beddoes CM, Case CP, Briscoe WH. Understanding nanoparticle cellular entry: a physicochemical perspective. Adv Colloid Interface Sci. 2015; 218: 48-68.
10.Yin Q, Shen J, Zhang Z, Yu H, Li Y. Reversal of multidrug resistance by stimuli-responsive drug delivery systems for therapy of tumor. Adv Drug Deliv Rev. 2013; 65(13): 1699-1715.
11.Davis ME, Shin DM. Nanoparticle therapeutics: an emerging treatment modality for cancer. Nat Rev Drug Discov. 2008; 7(9): 771-782.
12.Huwyler J, Cerletti A, Fricker G, Eberle AN, Drewe J. By-passing of P-glycoprotein using immunoliposomes. J Drug Target. 2002; 10(1): 73-79.
13.Rajagopal A, Simon SM. Subcellular localization and activity of multidrug resistance proteins. Mol Biol Cell. 2003; 14(8): 3389-3399.
14.Walker WA, Tarannum M, Vivero-Escoto JL. Cellular endocytosis and trafficking of cholera toxin B-modified mesoporous silica nanoparticles. J Mater Chem B. 2016; 4(7): 1254-1262.
15.Yang D, Wang T, Su Z, Xue L, Mo R, Zhang C. Reversing Cancer Multidrug Resistance in Xenograft Models via Orchestrating Multiple Actions of Functional Mesoporous Silica Nanoparticles. ACS Appl Mater Interfaces. 2016; 8(34): 22431-22441.
16.Ninomiya K, Kawabata S, Tashita H, Shimizu N. Ultrasound-mediated drug delivery using liposomes modified with a thermosensitive polymer. Ultrason Sonochem. 2014; 21(1): 310-316.
17.Mo R, Jiang T, Gu Z. Enhanced anticancer efficacy by ATP-mediated liposomal drug delivery. Angew Chem Int Ed Engl. 2014; 53(23): 5815-5820.
18.Dicheva BM, ten Hagen TL, Seynhaeve AL, Amin M, Eggermont AM, Koning GA. Enhanced specificity and drug delivery in tumors by cRGD-anchoring thermosensitive liposomes. Pharm Res. 2015; 32(12): 3862-3876.
19.Gao H, Zhang Q, Yu Z, He Q. Cell-penetrating peptide-based intelligent liposomal systems for enhanced drug delivery. Curr Pharm Biotechnol. 2014; 15(3): 210-219.
20.Moghadas-Sharif N, Fazly Bazzaz BS, Khameneh B, Malaekeh-Nikouei B. The effect of nanoliposomal formulations on Staphylococcus epidermidis biofilm. Drug Dev Ind Pharm. 2015; 41(3): 445-450.
21.Yazdani M, Jalali S, Badiee A, Shariat S, Mansourian M, Arabi L, Abbasi A, Saberi Z, Jaafari M. Stimulation of Tumor Specific Immunity by P5 HER-2/Neu Generatedpeptide Encapsulated in Nano-Liposomes with High Phase Transition Temperature Phospholipids. Curr Drug Deliv. 2016.
22.Ding J, Chen L, Xiao C, Chen L, Zhuang X, Chen X. Noncovalent interaction-assisted polymeric micelles for controlled drug delivery M. 2014; 50(77): 11274-11290.
23.Zhu L, Perche F, Wang T, Torchilin VP. Matrix metalloproteinase 2-sensitive multifunctional polymeric micelles for tumor-specific co-delivery of siRNA and hydrophobic drugs. Biomaterials. 2014; 35(13): 4213-4222.
24.Ke X-Y, Ng VWL, Gao S-J, Tong YW, Hedrick JL, Yang YY. Co-delivery of thioridazine and doxorubicin using polymeric micelles for targeting both cancer cells and cancer stem cells. Biomaterials. 2014; 35(3): 1096-1108.
25.Jhaveri AM, Torchilin VP. Multifunctional polymeric micelles for delivery of drugs and siRNA. Front Pharmacol. 2014; 5: 77.
26.Zhang C, Pan D, Luo K, Li N, Guo C, Zheng X, Gu Z. Dendrimer–doxorubicin conjugate as enzyme-sensitive and polymeric nanoscale drug delivery vehicle for ovarian cancer therapy. Polym Chem. 2014; 5(18): 5227-5235.
27.Yavuz B, Pehlivan SB, Vural İ, Ünlü N. In Vitro/In Vivo Evaluation of Dexamethasone—PAMAM Dendrimer Complexes for Retinal Drug Delivery. J Pharm Sci. 2015; 104(11): 3814-3823.
28.Chandra S, Noronha G, Dietrich S, Lang H, Bahadur D. Dendrimer-magnetic nanoparticles as multiple stimuli responsive and enzymatic drug delivery vehicle. J Magn Magn Mater. 2015; 380: 7-12.
29.Wu H, Shi H, Zhang H, Wang X, Yang Y, Yu C, Hao C, Du J, Hu H, Yang S. Prostate stem cell antigen antibody-conjugated multiwalled carbon nanotubes for targeted ultrasound imaging and drug delivery. Biomaterials. 2014; 35(20): 5369-5380.
30.Bhatnagar I, Venkatesan J, Kim S-K. Polymer functionalized single walled carbon nanotubes mediated drug delivery of gliotoxin in cancer cells. J Biomed Nanotechnol. 2014; 10(1): 120-130.
31.Al Faraj A, Shaik AP, Shaik AS. Magnetic single-walled carbon nanotubes as efficient drug delivery nanocarriers in breast cancer murine model: noninvasive monitoring using diffusion-weighted magnetic resonance imaging as sensitive imaging biomarker. Int J Nanomedicine. 2015; 10: 157.
32.Siu KS, Zheng X, Liu Y, Zhang Y, Zhang X, Chen D, Yuan K, Gillies ER, Koropatnick J, Min WP. Single-walled carbon nanotubes noncovalently functionalized with lipid modified polyethylenimine for siRNA delivery in vitro and in vivo. Bioconjug Chem. 2014; 25(10): 1744-1751.
33.Maleki Dizaj S, Barzegar-Jalali M, Zarrintan MH, Adibkia K, Lotfipour F. Calcium carbonate nanoparticles as cancer drug delivery system. Expert Opin Drug Deliv. 2015; 12(10): 1649-1660.
34.Elbialy NS, Fathy MM, Khalil WM. Doxorubicin loaded magnetic gold nanoparticles for in vivo targeted drug

delivery. Int J Pharm. 2015; 490(1): 190-199.
35.Qiu J, Zhang R, Li J, Sang Y, Tang W, Gil PR, Liu H. Fluorescent graphene quantum dots as traceable, pH-sensitive drug delivery systems. Int J Nanomedicine. 2015; 10: 6709.
36.You P, Yang Y, Wang M, Huang X, Huang X. Graphene oxide-based nanocarriers for cancer imaging and drug delivery. Curr Pharm Des. 2015; 21(22): 3215-3222.
37.Yang K, Feng L, Liu Z. Stimuli responsive drug delivery systems based on nano-graphene for cancer therapy. Adv Drug Deliv Rev. 2016; 105: 228-241.
38.Patel SC, Lee S, Lalwani G, Suhrland C, Chowdhury SM, Sitharaman B. Graphene-based platforms for cancer therapeutics. Ther Deliv. 2016; 7(2): 101-116.
39.Yahya Hanafi-Bojd M, Reza Jaafari M, Ramezanian N, Abnous K, Malaekeh-Nikouei B. Co-delivery of epirubicin and siRNA using functionalized mesoporous silica nanoparticles enhances in vitro and in vivo drug efficacy. Curr Drug Deliv. 2016; 13(7): 1176-1182.
40.Sadeghnia HR, Zoljalali N, Hanafi-Bojd MY, Nikoofal-Sahlabadi S, Malaekeh-Nikouei B. Effect of mesoporous silica nanoparticles on cell viability and markers of oxidative stress. Toxicol Mech Methods. 2015; 25(6): 433-439.
41.Hanafi-Bojd MY, Jaafari MR, Ramezanian N, Xue M, Amin M, Shahtahmassebi N, Malaekeh-Nikouei B. Surface functionalized mesoporous silica nanoparticles as an effective carrier for epirubicin delivery to cancer cells. Eur J Pharm Biopharm. 2015; 89: 248-258.
42.Ohta S, Yamura K, Inasawa S, Yamaguchi Y. Aggregates of silicon quantum dots as a drug carrier: selective intracellular drug release based on pH-responsive aggregation/dispersion. Chem Commun. 2015; 51(29): 6422-6425.
43.Zhou J, Zhang W, Hong C, Pan C. Silica nanotubes decorated by pH-responsive diblock copolymers for controlled drug release. ACS Appl Mater Interfaces. 2015; 7(6): 3618-3625.
44.Kresge C, Leonowicz M, Roth W, Vartuli J, Beck J. Ordered mesoporous molecular sieves synthesized by a liquid-crystal template mechanism. Nature. 1992; 359(6397): 710-712.
45.Vallet-Regi M, Ramila A, Del Real R, Pérez-Pariente J. A new property of MCM-41: drug delivery system. Chem Mater. 2001; 13(2):308-311.
46.Urata C, Aoyama Y, Tonegawa A, Yamauchi Y, Kuroda K. Dialysis process for the removal of surfactants to form colloidal mesoporous silica nanoparticles. Chem Commun. 2009 (34): 5094-5096.
47.Febvay S, Marini DM, Belcher AM, Clapham DE. Targeted cytosolic delivery of cell-impermeable compounds by nanoparticle-mediated, light-triggered endosome disruption. Nano Lett. 2010; 10(6): 2211-2219.
48.Mosallaei N, Jaafari MR, Hanafi-Bojd MY, Golmohammadzadeh S, Malaekeh-Nikouei B. Docetaxel-loaded solid lipid nanoparticles: Preparation, characterization, in vitro, and in vivo evaluations. , J Pharm Sci. 2013; 102(6): 1994-2004.
49.Slowing II, Vivero-Escoto JL, Wu C-W, Lin VS-Y. Mesoporous silica nanoparticles as controlled release drug delivery and gene transfection carriers. Adv Drug Deliv Rev. 2008; 60(11): 1278-1288.
50.Slowing II, Trewyn BG, Lin VS-Y. Mesoporous silica nanoparticles for intracellular delivery of membrane-impermeable proteins. J Am Chem Soc. 2007; 129(28): 8845-8849.
51.Vivero-Escoto JL, Slowing II, Lin VS-Y. Tuning the cellular uptake and cytotoxicity properties of oligonucleotide intercalator-functionalized mesoporous silica nanoparticles with human cervical cancer cells HeLa. Biomaterials. 2010; 31(6): 1325-1333.
52.Gao Y, Chen Y, Ji X, He X, Yin Q, Zhang Z, Shi J, Li Y. Controlled intracellular release of doxorubicin in multidrug-resistant cancer cells by tuning the shell-pore sizes of mesoporous silica nanoparticles. ACS Nano. 2011; 5(12): 9788-9798.
53.Rosenberg MF, Kamis AB, Callaghan R, Higgins CF, Ford RC. Three-dimensional structures of the mammalian multidrug resistance P-glycoprotein demonstrate major conformational changes in the transmembrane domains upon nucleotide binding. J Biol Chem. 2003; 278(10): 8294-8299.
54.Rosenberg MF, Callaghan R, Modok S, Higgins CF, Ford RC. Three-dimensional Structure of P-glycoprotein The transmembrane regions adopt an asymmetric configuration in the nucleotide-bound state. J Biol Chem. 2005; 280(4):2857-2862.
55.Loo TW, Clarke DM. Determining the dimensions of the drug-binding domain of human P-glycoprotein using thiol cross-linking compounds as molecular rulers. J Biol Chem. 2001; 276(40): 36877-36880.
56.Dong Y, Yang J, Liu H, Wang T, Tang S, Zhang J, Zhang X. Site-specific drug-releasing polypeptide nanocarriers based on dual-pH response for enhanced therapeutic efficacy against drug-resistant tumors. Theranostics. 2015; 5(8): 890.
57.Moon YJ, Morris ME. Pharmacokinetics and bioavailability of the bioflavonoid biochanin A: effects of quercetin and EGCG on biochanin A disposition in rats. Mol Pharm. 2007; 4(6): 865-872.
58.Jin W, Liu Y, Xu S-g, Yin W-j, Li J-j, Yang J-m, Shao Z-m. UHRF1 inhibits MDR1 gene transcription and sensitizes breast cancer cells to anticancer drugs. Breast Cancer Res Treat. 2010; 124(1): 39-48.
59.Grandi M, Geroni C, Giuliani F. Isolation and characterization of a human colon adenocarcinoma cell line resistant to doxorubicin. Br J Cancer. 1986; 54(3): 515.
60.Zhang X, Yashiro M, Qiu H, Nishii T, Matsuzaki T, Hirakawa K. Establishment and characterization of multidrug-resistant gastric cancer cell lines. Anticancer Res. 2010; 30(3): 915-921.